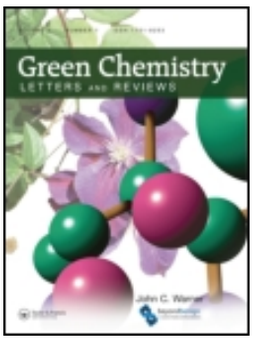

Green Chemistry Letters and Reviews

ISSN: 1751-8253 (Print) 1751-7192 (Online) Journal homepage: http://www.tandfonline.com/loi/tgcl20

Development of novel graphene-like layered hexagonal boron nitride for adsorptive removal of antibiotic gatifloxacin from aqueous solution

Yanhong Chao, Wenshuai Zhu, Jiaxin Chen, Peiwen Wu, Xiangyang Wu, Huaming Li, Changri Han & Shan Yan

To cite this article: Yanhong Chao, Wenshuai Zhu, Jiaxin Chen, Peiwen Wu, Xiangyang Wu, Huaming Li, Changri Han & Shan Yan (2014) Development of novel graphene-like layered hexagonal boron nitride for adsorptive removal of antibiotic gatifloxacin from aqueous solution, Green Chemistry Letters and Reviews, 7:4, 330-336, DOI: 10.1080/17518253.2014.944941

To link to this article: https://doi.org/10.1080/17518253.2014.944941

Published online: 21 Aug 2014.

Green Chemistry Letters and Reviews, 2014
Vol. 7, No. 4, 330–336, http://dx.doi.org/10.1080/17518253.2014.944941

Taylor & Francis
Taylor & Francis Group

RESEARCH LETTER

Development of novel graphene-like layered hexagonal boron nitride for adsorptive removal of antibiotic gatifloxacin from aqueous solution

Yanhong Chao[a,b]*, Wenshuai Zhu[c], Jiaxin Chen[b], Peiwen Wu[c], Xiangyang Wu[a]*, Huaming Li[c], Changri Han[d] and Shan Yan[e]

[a]*School of the Environment, Jiangsu University, Zhenjiang, P.R. China;* [b]*School of Pharmacy, Jiangsu University, Zhenjiang, P.R. China;* [c]*School of Chemistry and Chemical Engineering, Jiangsu University, Zhenjiang, P.R. China;* [d]*Key Laboratory of Tropical Medicinal Plant Chemistry of Education, Hainan Normal University, Haikou, P.R. China;* [e]*Zhenjiang Institute of Environmental Science, Zhenjiang, P.R. China*

(*Received 20 November 2013; final version received 11 July 2014*)

Graphene-like layered hexagonal boron nitride (*g*-BN) was prepared and characterized. The performance of using *g*-BN as an adsorbent for removal of fluoroquinolone antibiotic gatifloxacin (GTF) from aqueous solution was evaluated. *g*-BN showed an excellent adsorption capability with notable GTF adsorption ratio of more than 90%. Data of equilibrium adsorption of GTF onto *g*-BN at different temperatures were represented by Langmuir, Freundlich and Tempkin isotherm models, and Langmuir exhibited the best fitting with the maximum adsorption capacity of 88.5 $mg{\cdot}g^{-1}$ at 288 K. GTF adsorption was insignificantly affected by solution pH. Competitive role of Na^+ and Ca^{2+} in the solution inhibited the adsorption of GTF and decreased the adsorption capacity a bit. The adsorption process was spontaneous and exothermic. The adsorption was probably governed by π–π interaction between GTF and *g*-BN, and electrostatic interaction may also exist in the adsorption process.

Keywords: graphene-like boron nitride; adsorptive removal; antibiotics; gatifloxacin

1. Introduction

Pharmaceutical antibiotics have been extensively used in human therapy and the farming industry because of their specific antimicrobial activities. Recent years, the presence of antibiotics in aquatic environment has attracted increasing concern and these antibiotics have been proved as a new class of potent contaminants. Antibiotics are difficult to be degraded, and the degradation byproducts may be even more toxic than their parent compounds (*1*). Residues of these antibiotics are frequently detected in soil, groundwater, surface water, and even drinking water in $ng{\cdot}L^{-1}$ –$\mu g{\cdot}L^{-1}$ range all over the world (*2*). They have created severe potential risks to human and ecological health (*3*). The spread of antibiotic resistance among bacterial populations is a typical issue elicited by the widespread use of antibiotics. Specifically, the fluoroquinolone antibiotics, which are poorly metabolized, have been shown to disrupt microbial respiration. The removal of fluoroquinolone antibiotics by conventional water and wastewater treatment technologies is generally incomplete (*4*). By now, many methods such as chemical oxidation, biodegradation, photodegradation, membrane filtration, and adsorption have been developed (*5–7*). And adsorption has been considered to be an attractive and effective technology for removal of these organic pollutants. Recently, a great deal of adsorbents has been investigated and shown good potential, for example, graphene oxide (*8–10*), carbon nanotubes (*11–13*), activated carbon (*14–16*), mesoporous nanocomposite (*17*), porous resins (*12*), montmorillonite (*18*), bentonite (*19*), and kaolinite (*20*). Table 1 lists some of these adsorbents for removal of common antibiotics pollutants in water. The single-walled carbon nanotubes (SWNTs) showed much better adsorption capacity than the multi-walled carbon nanotubes (MWNT) due to their higher surface area. Layered graphene oxide and its modified composites also displayed good potential for adsorptive removal of antibiotics. Moreover, in these studies, adsorption was found to be primarily driven by the functionalities of the antibiotic molecules, the spatial structure or active sites of the adsorbents, pH conditions, and ionic level of adsorption system. Nevertheless, the development of efficient adsorbents with their adsorption mechanism still needs more attention.

*Corresponding authors. Emails: chaoyh@ujs.edu.cn; wuxy@ujs.edu.cn

Table 1. The adsorption capacity of various adsorbents for antibiotics removal.

Adsorbents	Antibiotics	q_{max}[a] (mg/g)	S_{BET} (m^2/g)	Dose (g/L)	$C_{0,max}$ (mg/L)	t(h)	pH	T(K)	Refs.
Graphene oxide	Tetracycline	313	/	0.18	333	Overnight	3.6	298	(*9*)
rGO-M[b]	Ciprofloxacin	19	/	0.2	10	24	6.2	298	(*8*)
rGO-M[b]	Norfloxacin	23	/	0.2	10	24	6.2	298	(*8*)
Fe_3O_4–rGO	Tetracycline	95	/	1.6	75	24	/	298	(*10*)
Ac[c,1]	Cephalexin	66	1032	0.4	32	60	/	293	(*15*)
Ac[1]–Cu(II)	Cephalexin	78	1030	0.4	32	60	/	293	(*15*)
Ac[1]–Fe(III)	Cephalexin	75	939	0.4	32	60	/	293	(*15*)
Ac[2]–K_2CO_3	Cephalexin	118	1677	0.5	100	1.5	7	303	(*16*)
MWNT[d]	Norfloxacin	89	160	0.5	100	10	7	318	(*12*)
MWNT[d]	Tetracycline	100	148	0.38	84	84	6	298	(*13*)
SWNT[e]	Tetracycline	340	370	0.38	84	84	5.7	298	(*13*)

[a]The maximum adsorption capacity.
[b]Reduced graphene oxide/magnetite composite.
[c]Activated carbon; [1]from lotus stalks; [2]from *Albizia lebbeck* seed pods.
[d]Multi-walled carbon nanotubes.
[e]Single-walled carbon nanotubes.

Recently, layered materials have attracted more and more attentions due to the large specific surface area and excellent adsorption ability. Among layered materials, graphene-like layered hexagonal boron nitride (*g*-BN), isoelectronic to the similarly structured carbon lattice, has gained much attention because of high temperature stability, outstanding mechanical strength, and high corrosion resistance, resulting in a series of potential applications as an excellent adsorbent. As a layered material, the number of layers of *g*-BN has an important effect on its specific surface area, further affect the adsorptive capability.

Herein, the *g*-BN was synthesized and applied in adsorptive removal of gatifloxacin (GTF) from aqueous solution. The adsorption characteristics and mechanisms of a representative fluoroquinolone antibiotic, GTF, were investigated in batch adsorption experiments. The structure of GTF was shown in Figure 1. The impacts of pH, ionic strength, and temperature on adsorption were studied, and the adsorption isotherms and thermodynamics were evaluated.

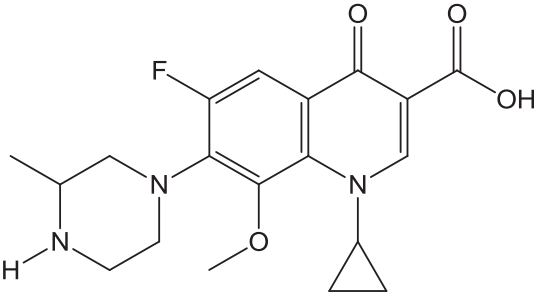

Figure 1. The structure of gatifloxacin.

2. Experimental

2.1. Materials and instrumentation

All chemicals used were of analytical reagent grade and used without further purification. GTF was obtained from Sigma–Aldrich Chemical Co. (99% purity). The commercial BN powder was purchased from Sinopharm Chemical Reagent Co. Ltd. (China). *g*-BN was prepared as described by Nag et al. (*21*).

2.2. Adsorption of GTF by g-BN

The adsorption experiments were carried out in 50-mL conical flasks which were wrapped with aluminum foils to avoid possible photodegradation of GTF. Ten milliliter of 80 ± 1 mg·L^{-1} GTF solution and 10 ± 0.2 mg *g*-BN powder were introduced into the flasks and mixed thoroughly by a vortex mixer for a few seconds. The suspension was mounted in a thermostatic shaker bath with a shaking speed of 130 rpm at a preset temperature of 298 K for adsorption. After shaking 15 min, the adsorption equilibrium reached, and the suspension was centrifuged at 20,000 rpm for 10 min. Then the supernatant was collected and analyzed immediately by UV–Vis spectrophotometer at 286 nm. Unless noted specifically, the following adsorption experiments were performed under the same condition. To study the impact of pH on adsorption, the pH of GTF solution was adjusted from 3 to 11 using 0.02 mol·L^{-1} NaOH or HCl. To investigate the effect of ionic strength on adsorption, different amounts of NaCl or $CaCl_2$ were dissolved in the mixture to get the ionic strength in the range of 0–1.37 mol·L^{-1}. Adsorption isotherm and thermodynamic studies were carried out with initial GTF concentrations of 20–80 mg·L^{-1} at controlled

temperatures of 288, 303 and 318 K. Adsorption data were collected in triplicate for each experiment. A linear calibration curve (absorbance versus concentration) of $A = 0.0592\ C + 0.0051$ ($R^2 = 0.999$) was used to determine the concentration of GTF. The adsorption capacity, q_e ($mg \cdot g^{-1}$), was calculated using Equation (1)

$$q_e = V(C_0 - C_e) / m \quad (1)$$

where C_0 is the initial GTF concentration ($mg \cdot L^{-1}$), C_e is the residual GTF concentration at equilibrium ($mg \cdot L^{-1}$), V is the volume of solution (L), and m is the mass of dry *g*-BN (g).

3. Results and discussion

3.1. Adsorption properties of as-prepared adsorbent g-BN for GTF

The adsorption properties of *g*-BN we synthesized above and the purchased commercial BN were compared under the same adsorption condition in this study. As shown in Figure 2, the adsorption performance of *g*-BN was obviously much better than that of commercial BN. More than 90% GTF were removed in 15 min when selecting *g*-BN as an adsorbent, while commercial BN displayed only less than 10% GTF removal. This result predicted that the prepared *g*-BN might have excellent adsorption potency for the removal of antibiotic GTF from water.

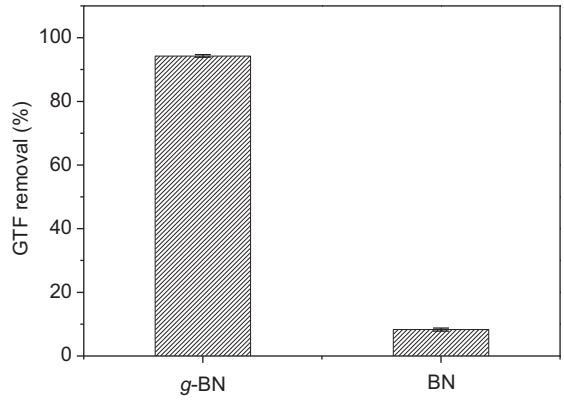

Figure 2. Adsorption comparison of *g*-BN and BN ($m_{sorbent}$ = 10 mg; C_0 = 80 $mg \cdot L^{-1}$; 15 min; 298 K).

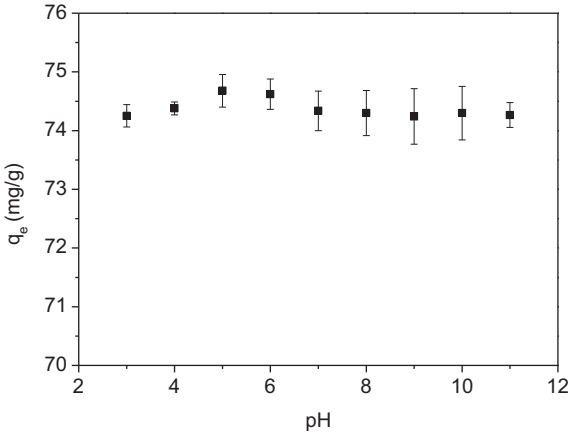

Figure 3. Effect of pH for GTF adsorption onto *g*-BN ($m_{sorbent}$ = 10 mg; C_0 = 80 $mg \cdot L^{-1}$; 15 min; 298 K).

3.2. Effect of pH on GTF adsorption

The effect of solution pH on the adsorption of GTF onto *g*-BN was investigated in the range of pH 3–11, and the results were described in Figure 3. It was found that GTF adsorption onto *g*-BN hardly depended on the solution pH. Although the optimal pH for the adsorption was pH 5–6 seen from Figure 3, the pH effect was generally insignificant for the adsorption of GTF. The *g*-BN can effectively remove GTF in a wide range of pH 3–11 with an average high adsorption capacity of 74.4 ± 0.3 $mg \cdot g^{-1}$.

As is well known, π–π interaction as a dominant driving force has always been used to explain the mechanism of aromatic adsorbate to layered graphene surface (*8*, *9*). The adsorbent *g*-BN has a virtual orbital of B, presenting some Lewis acidity, which can be as electron acceptor. And the adsorbate GTF has two aromatic rings in the structure which can be as π electron donor. There was no observable effect on GTF adsorption with pH changing from 3 to 11, which was probably due to the π–π interaction between the adsorbate and the adsorbent. The non-electrostatic interaction of π–π dispersion may dominate the adsorption of GTF onto *g*-BN. In order to verify this assumption, the occupied area of per adsorbed GTF molecule on the adsorbent *g*-BN, *Am* ($Å^2$), is calculated by the following equation:

$$Am = \frac{(S_{BET} \times M_W)}{(q_m \times N_A)} \quad (2)$$

where S_{BET} is the Brunauer–Emmett–Teller (BET) surface area ($m^2 \cdot g^{-1}$) of *g*-BN, which is determined as 167 $m^2 \cdot g^{-1}$; M_w is the molecular weight of GTF; N_A is the Avogadro constant; and q_m is the maximum amount absorbed per unit weight of the *g*-BN ($mg \cdot g^{-1}$), which is approximately 74.4 $mg \cdot g^{-1}$ in the range of pH 3–11 at 298 K. The *Am* value obtained is about 140 $Å^2$ for per GTF molecule on *g*-BN. It is known that a typical area per molecule for an alkane on similar substrates is about 60–70 $Å^2$ for decane and about 90–100 $Å^2$ for

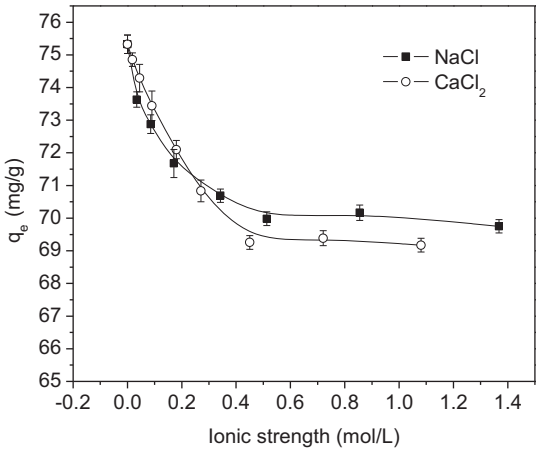

Figure 4. Effect of ionic strength of NaCl and $CaCl_2$ for GTF adsorption onto *g*-BN ($m_{sorbent}$ = 10 mg; C_0 = 80 mg·L^{-1}; 15 min; 298 K).

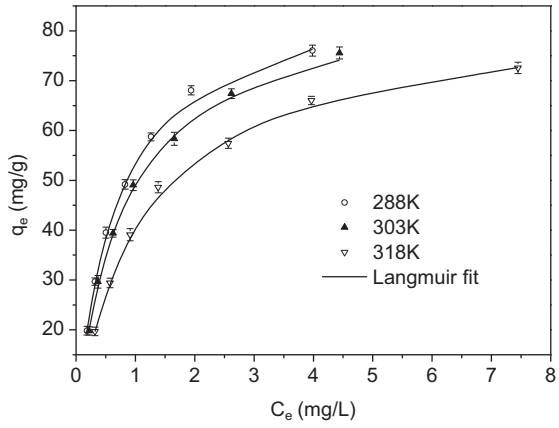

Figure 5. Adsorption isotherms for GTF adsorption onto *g*-BN fitting by Langmuir model ($m_{sorbent}$ = 10 mg; C_0 = 20–80 mg·L^{-1}; 15 min).

hexadecane. So it can be revealed that the GTF molecules ($C_{19}H_{22}FN_3O_4$) are lying flat on the surface of *g*-BN, and the π–π interaction between GTF and *g*-BN is indeed exist and play an important role during the adsorption.

3.3. Effect of ionic strength on GTF adsorption

To study the effect of ionic strength on the adsorption of GTF onto *g*-BN, different amounts of NaCl or $CaCl_2$ were added to the solution. The results are shown in Figure 4. The adsorption capacity of GTF decreased as the ionic strength increased. For NaCl, the adsorption capacity decreased obviously with the addition of NaCl increasing from 0 to 0.34 mol·L^{-1}, then the adsorption capacity decreased slowly and had no observable change with further increasing NaCl to 1.37 mol·L^{-1}. The effect of $CaCl_2$ on the adsorption was similar to that of NaCl and displayed an inhibitory effect for GTF adsorption onto *g*-BN. The adsorption capacity declined from 75.3 ± 0.3 to 70.8 ± 0.3 mg·g^{-1} as the concentration of $CaCl_2$ increased from 0 to 0.27 mol·L^{-1}. Then further increasing $CaCl_2$ to 1.08 mol·L^{-1}, the adsorption capacity declined slowly and reached a plateau at 69.3 ± 0.2 mg·g^{-1}. As shown in Figure 4, the variation of the adsorption capacity stops and is thereafter constant as NaCl or $CaCl_2$ in the solution was about 0.5 mol·L^{-1}. The adsorption capacity of GTF generally declined by 7 ± 1% and 8 ± 1% for the increase of NaCl and $CaCl_2$, respectively. This result suggested that the electrostatic competition existed and played a certain role during the adsorption process. And there was no significant difference in the competitive inhibition of Na^+ and Ca^{2+} in the solution for the adsorption.

3.4. GTF adsorption isotherms

The equilibrium isotherms at various temperatures were studied by varying the initial concentration of GTF. Adsorption isotherms plotted as adsorbed amount (q_e, mg·g^{-1}) versus equilibrium aqueous-phase concentrations (C_e, mg·L^{-1}) at 288, 303, and 318 K were presented in Figure 5. An obviously more adsorption could be seen as the temperature decreased from 318 K to 288 K, indicating that the adsorption was exothermic and favored at lower temperatures.

The adsorption isotherms are significant for predicting the maximum adsorption capacity and describing the surface properties and affinity of the adsorbent (*10*). In this study, three widely used isotherm models: Langmuir (*22*), Freundlich (*23*), and Tempkin (*24*) models were selected to analyze the equilibrium data for the adsorption of GTF onto *g*-BN.

$$\text{Langmuir isotherm}\quad q_e = q_m \frac{K_L C_e}{1 + K_L C_e} \tag{3}$$

$$\text{Freundlich isotherm}\quad q_e = K_F C_e^{1/n} \tag{4}$$

$$\text{Tempkin isotherm}\quad q_e = B\ln K_T + B\ln C_e \tag{5}$$

where q_m (mg·g^{-1}) is the theoretical maximum adsorption capacity, K_L (L·mg^{-1}) is the Langmuir constant related to the affinity of binding sites, K_F (mg·g^{-1}) and n are Freundlich constants which give a measure of adsorption capacity and intensity, respectively, K_T

($L \cdot mg^{-1}$) is Tempkin constant corresponded to the maximum binding energy, and B is Tempkin constant related to the heat of sorption. Langmuir model is an ideal model, which assumes that the surface of the adsorbent is uniform and can only be covered with a complete monolayer, all the adsorption sites are equivalent, and adsorbed molecules do not interact with each other. Freundlich model is a widely used empirical equation which based on adsorption on heterogeneous surface with a non-uniform distribution of adsorption heat and affinities through a multilayer adsorption, while Tempkin model is a proper model for chemical adsorption based on strong electrostatic interaction between positive and negative charges (*9*). Furthermore, the average percentage error (APE) was used to illustrate the best model to describe the adsorption. APE can be calculated by the following equation:

$$\text{APE}\ (\%) = \frac{\sum_{i=1}^{N} \left| (q_{e,\exp} - q_{e,\text{cal}})/(q_{e,\exp}) \right|}{N} \times 100 \quad (6)$$

where N is the number of experimental data points.

The fitted results of three isotherm models and the APE (%) values at different temperatures are presented in Table 2. The results showed that the correlation of isotherms was in the order: Langmuir > Tempkin > Freundlich for GTF adsorption onto *g*-BN. Langmuir model displayed the best fitting for the equilibrium data with the high correlation coefficient values (R^2 > 0.9992) and low APE (%). This result implied the monolayer adsorption nature of GTF, which may be due to the homogeneous distribution of active sites on the surface of prepared *g*-BN. However, considering the limited solubility of GTF in water, the maximum concentration of GTF we studied in the isotherm was 80 $mg \cdot L^{-1}$, which resulted in certain limitations in this hypothesis of monolayer adsorption. Multi-layering adsorption might also be displayed if the studied concentration of GTF could be increased much more higher.

As shown in Table 2, the Langmuir maximum adsorption capacity was 88.5 $mg \cdot g^{-1}$ for GTF at 288 K. Comparing with the adsorbents listed in Table 1, the q_{max} of *g*-BN was higher than the grapheme oxide/magnetite composites and the Cu(II)/Fe(III) impregnated activated carbons, but seemed not as good as the grapheme oxide and the SWNTs. But considering the fact that the magnitude of q_{max} was also influenced by the adsorbent dose, the maximum initial concentration of adsorbate, and some other conditions during the isotherm study, this comparison only based on q_{max} was actually imperfect and some other study conditions listed in Table 1 also should be taken into account. So the adsorption capacity of *g*-BN for

Table 2. Adsorption isotherm parameters for GTF adsorption onto *g*-BN.

	Langmuir					Freundlich				Tempkin			
T (K)	K_L ($L \cdot mg^{-1}$)	q_m ($mg \cdot g^{-1}$)	R_L	R^2	APE (%)	K_F ($mg \cdot g^{-1}$)	$1/n$	R^2	APE (%)	K_T ($L \cdot mg^{-1}$)	B	R^2	APE (%)
288	1.57	88.50	0.01–0.03	0.9997	0.83	48.70	0.44	0.9448	9.29	15.66	19.12	0.9916	2.47
303	1.38	86.21	0.01–0.04	0.9992	1.26	44.53	0.44	0.9567	7.91	13.33	18.78	0.9986	1.22
318	0.98	82.65	0.01–0.05	0.9995	1.04	36.94	0.41	0.9390	8.98	10.29	17.35	0.9911	3.25

Note: All isotherm parameters shown in this table have a relative standard deviation less than ± 5%.

GTF was good and *g*-BN had potential for antibiotics removal from wastewater.

The essential characteristics of the Langmuir isotherm can be expressed by means of a dimensionless constant separation factor R_L ($R_L = 1/(1 + K_L C_0)$). The R_L values listed in Table 2 were found to be between 0 and 1, which indicated that the adsorption process was quite favorable (*10*). The conclusion of the favorable adsorption process also could be obtained on the basis of Freundlich constant $1/n$ values, which were less than 1 at all temperatures (*25*). Tempkin model gave a good fit on GTF adsorption onto *g*-BN, which suspected that there was electrostatic interaction in the process of adsorption. This presume can be confirmed by the sequitur deduced from the impact study of ionic strength.

3.5. GTF adsorption thermodynamics

The feature of the adsorption process can be interpreted by thermodynamic analysis from the aspect of energy change. The thermodynamic feasibility for the adsorption of GTF onto *g*-BN has been demonstrated by the evaluation of thermodynamic parameters including the entropy ($\Delta S°$), the enthalpy ($\Delta H°$), and the Gibbs free energy ($\Delta G°$), which are calculated by the following equations:

$$\ln K_c = \frac{\Delta S^\circ}{R} - \frac{\Delta H^\circ}{RT} \quad (7)$$

$$\Delta G^\circ = -RT \ln K_c \quad (8)$$

where R is the ideal gas constant ($J \cdot mol^{-1} \cdot K^{-1}$); T is the temperature (K); K_c is the equilibrium distribution coefficient, which is the ratio of the amount adsorbed on solid to the equilibrium concentration in solution. The values of $\Delta S°$ and $\Delta H°$ can be calculated from the intercept and the slope of the linear plots of $\ln Kc$ vs. $1/T$ (Figure 6). The estimated $\Delta S°$ value was about –0.02 ± 0.003 $kJ \cdot mol^{-1} \cdot K^{-1}$, and the $\Delta H°$ value was about −16.51 ± 0.6 $kJ \cdot mol^{-1}$. The negative value of $\Delta H°$ revealed the exothermic nature of GTF adsorption onto *g*-BN (*16*). The values of $\Delta G°$ calculated by Equation (8) at 288, 303, and 318 K were −10.95 ± 0.23, −10.95 ± 0.26, and −10.36 ± 0.32 $kJ \cdot mol^{-1}$, respectively. These values were all negative and in the range of –20 to 0 $kJ \cdot mol^{-1}$, indicating that the adsorption of GTF onto *g*-BN may be a spontaneous and physisorption process (*26*, *27*).

3.6. Investigation of the stability and solubility of g-BN

The fresh *g*-BN and reclaimed *g*-BN were measured by X-ray diffraction (XRD) using D8 Advance X-ray diffraction. XRD of the fresh *g*-BN and reclaimed *g*-BN is given in Figure 7. The results indicated that *g*-BN was stable in the reaction process. To investigate whether the BN was leached into the aqueous, the *B*-content determination in water sample has been carried out by atomic emission spectrometry with inductively coupled plasma optical emission spectrometer (ICP-OES). After reaction, the water sample was directly determined. The *B* content was detected less than 0.02 $mg \cdot L^{-1}$ in water. This result indicated that the proportion of *g*-BN leached into the water phase was negligible.

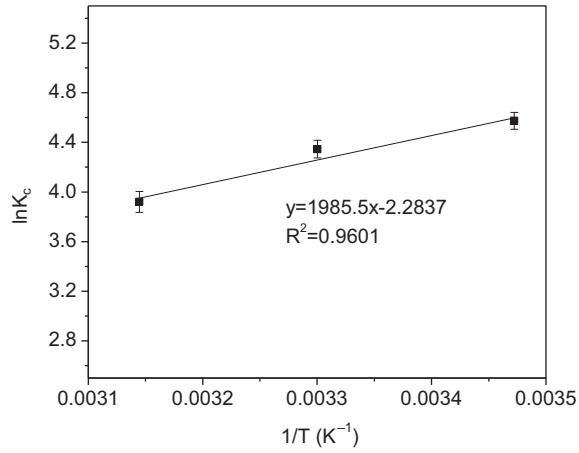

Figure 6. The thermodynamics for GTF adsorption onto *g*-BN based on Equation (*7*).

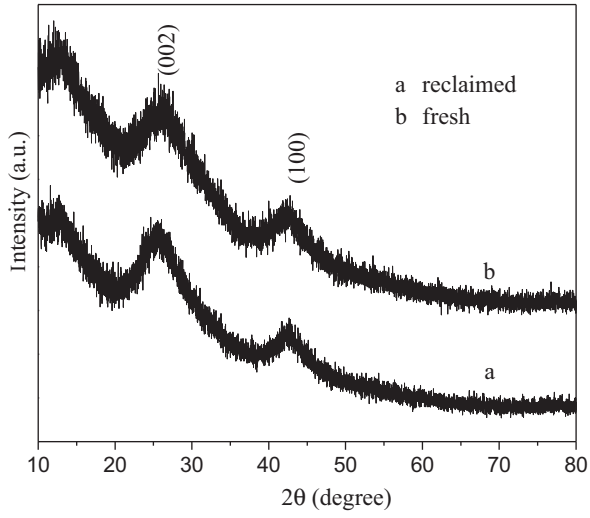

Figure 7. XRD of fresh *g*-BN and reclaimed *g*-BN.

4. Conclusions

In this study, *g*-BN has been prepared, characterized, and investigated the adsorption behavior for the

commonly used fluoroquinolone antibiotic GTF. Comparing with commercial BN, the prepared *g*-BN demonstrated a much better capability in the removal of GTF from aqueous solution with excellent GTF adsorption ratio of more than 90%. The effect of pH on the adsorption was generally not observable, and the average adsorption capacity could reach 74.4 ± 0.3 $mg \cdot g^{-1}$ in a wide range of pH 3–11. The ionic strength with 0–1.37 $mol \cdot L^{-1}$ NaCl and $CaCl_2$ in the solution inhibited the adsorption of GTF onto *g*-BN with decreasing by 7 ± 1% and 8 ± 1% adsorption capacity, respectively. Equilibrium adsorption data were well described by Langmuir isotherm model, showing the maximum adsorption capacity of 88.5 $mg \cdot g^{-1}$ at 288 K. The adsorption was a spontaneous and exothermic process. π–π interaction may dominate the adsorption of GTF onto *g*-BN, and the electrostatic interaction may also play a certain role during the adsorption process.

Funding

This work was financially supported by the National Nature Science Foundation of China [grant numbers 21376111, 21276117, and 21166009], Natural Science Foundation of Jiangsu Province [grant number BK20130513], Society Development Fund of Zhenjiang [grant number SH2012009], and Doctoral Innovation Fund of Jiangsu Province [grant number CXLX12_0667].

References

(1) Wang, X.H.; Lin, A.Y.C. *Environ. Sci. Technol*. **2012**, *46*, 12417.
(2) Homem, V.; Santos, L. *J. Environ. Manag*. **2011**, *92*, 2304.
(3) Baquero, F.; Martinez, J.L.; Canton, R. *Curr. Opin. Biotechnol*. **2008**, *19*, 260.
(4) Zhou, L.J.; Ying, G.G.; Liu, S.; Zhao, J.L.; Yang, B.; Chen, Z.F.; Lai, H.J. *Sci. Total Environ*. **2013**, *452*, 365.
(5) Kummerer, K. *Chemosphere* **2009**, *75*, 435.
(6) Van Doorslaer, X.; Heynderickx, P.M.; Demeestere, K.; Debevere, K.; Van Langenhove, H.; Dewulf, J. *Appl. Catal. B-Environ*. **2012**, *111*, 150.
(7) Laera, G.; Cassano, D.; Lopez, A.; Pinto, A.; Pollice, A.; Ricco, G.; Mascolo, G. *Environ. Sci. Technol*. **2012**, *46*, 1010.
(8) Tang, Y.L.; Guo, H.G.; Xiao, L.; Yu, S.L.; Gao, N.Y.; Wang, Y.L. *Colloids Surf. A* **2013**, *424*, 74.
(9) Gao, Y.; Li, Y.; Zhang, L.; Huang, H.; Hu, J.J.; Shah, S.M.; Su, X.G. *J. Colloid Interface Sci*. **2012**, *368*, 540.
(10) Huang, L.H.; Sun, Y.Y.; Wang, W.L.; Yue, Q.Y.; Yang, T. *Chem. Eng. J*. **2011**, *171*, 1446.
(11) Peng, H.B.; Pan, B.; Wu, M.; Liu, Y.; Zhang, D.; Xing, B.S. *J. Hazard. Mater*. **2012**, *233*, 89.
(12) Yang, W.B.; Lu, Y.P.; Zheng, F.F.; Xue, X.X.; Li, N.; Liu, D.M. *Chem. Eng. J*. **2012**, *179*, 112.
(13) Ji, L.L.; Chen, W.; Duan, L.; Zhu, D.Q. *Environ. Sci. Technol*. **2009**, *43*, 2322.
(14) Liu, W.F.; Zhang, J.; Zhang, C.L.; Ren, L. *Chem. Eng. J*. **2011**, *171*, 431.
(15) Liu, H.; Liu, W.F.; Zhang, J.A.; Zhang, C.L.; Ren, L.; Li, Y. *J. Hazard. Mater*. **2011**, *185*, 1528.
(16) Ahmed, M.J.; Theydan, S.K. *Chem. Eng. J*. **2012**, *211–212*, 200.
(17) Shi, S.; Fan, Y.W.; Huang, Y.M. *Ind. Eng. Chem. Res*. **2013**, *52*, 2604.
(18) Wu, Q.F.; Li, Z.H.; Hong, H.L.; Yin, K.; Tie, L.Y. *Appl. Clay Sci*. **2010**, *50*, 204.
(19) Al-Khalisy, R.S.; Al-Haidary, A.M.A.; Al-Dujaili, A.H. *Sep. Sci. Technol*. **2010**, *45*, 1286.
(20) Li, Z.H.; Hong, H.L.; Liao, L.B.; Ackley, C.J.; Schulz, L.A.; MacDonald, R.A.; Miheliche, A.L.; Emard, S.M. *Colloid Surf. B*. **2011**, *88*, 339.
(21) Nag, A.; Raidongia, K.; Hembram, K.P.S.S.; Datta, R.; Waghmare, U.V.; Rao, C.N.R. *ACS Nano* **2010**, *4*, 1539.
(22) Langmuir, I. *J. Am. Chem. Soc*. **1916**, *38*, 2221.
(23) Freundlich, H.M.F. *J. Phys. Chem*. **1906**, *57*, 385.
(24) Tempkin, M.I.; Pyzhev, V. *Acta Physiochim. U.R.S.S*. **1940**, *12*, 327.
(25) Putra, E.K.; Pranowo, R.; Sunarso, J.; Indraswati, N.; Ismadji, S. *Water Res*. **2009**, *43*, 2419.
(26) Zhang, D.; Niu, H.Y.; Zhang, X.L.; Meng, Z.F.; Cai, Y.Q. *J. Hazard. Mater*. **2011**, *192*, 1088.
(27) Bekci, Z.; Seki, Y.; Yurdakoc, M.K. *J. Mol. Struct*. **2007**, *827*, 67.